Analysis of 21cm Radiation and the Galactic Rotational Curve using the TLM18 Radio Telescope

Jiarui Zhao *

Dulwich College Beijing, China

* Corresponding Author Email: 350277208@qq.com

Abstract. The galaxy has always been an unknown place for humans. Despite the advancement of modern technologies, it is still very hard for scientists to determine the entities that exist in space. The 21-cm radiation is electromagnetic radiation emitted by neutral hydrogen atoms undergoing a specific energy transition. In this research project, the aim is to understand the usage of the TLM-18 radio telescope in analyzing data from drift scans, including Sun scans, Cas A-scans, and the 21 cm radiation. We will also determine a galactic rotation curve for our galaxy. The Milky Way data is collected using the 18m TLM18 radio telescope located in Belmar, New Jersey, USA. The data are then interpreted in Matplotlib to generate line graphs and heatmaps that reveal patterns within space, such as galactic rotation. This project serves as a model for analyzing and interpreting data from the telescope. The data is visualized using Python libraries to enhance the visual representation and facilitate a more comprehensive examination.

Keywords: 21-cm radiation, TLM-18 radio telescope, drift scans, Sun scans, Cas A, galactic rotation, Python, Matplotlib.

1. Introduction

1.1. Background

Dark matter, 21cm radiation, and rotation curves are three fascinating phenomena in the field of physics that have attracted significant attention and research. Each of these areas offers unique insights into the fundamental nature of the universe, challenging our current understanding and driving scientific exploration.

Dark matter is a mysterious substance that exists throughout the universe and significantly impacts the formation and development of galaxies. Even though it cannot be seen or directly detected, its presence is inferred based on its gravitational influence on visible matter. The elusive nature of dark matter has led to extensive research efforts aimed at understanding its composition, characteristics, and role within the cosmic framework [1,2].

The study of 21cm radiation emitted during the transition of neutral hydrogen atoms provides a valuable tool for probing the early universe and the distribution of matter. By examining variations and absorption patterns in the 21cm radiation, scientists can acquire valuable knowledge about the development of cosmic structures, the interaction between visible matter and dark matter, and the overall progression of the universe [3,4].

By studying the fluctuations and absorption patterns present in the 21cm radiation, researchers can obtain valuable insights into the formation and evolution of cosmic structures and the characteristics of galactic rotational curves. Analyzing these patterns provides a deeper understanding of how galaxies rotate and the mass distribution within them, thus letting us understand how the universe functions [5,6].

1.2. Context

The 21 cm radiation refers to the electromagnetic radiation emitted by neutral hydrogen atoms transitioning between two energy states. It has a specific wavelength of electromagnetic radiation emitted by neutral hydrogen atoms undergoing a spin-flip transition [7]. Unlike the photons emitted during the main atomic transitions in hydrogen, which have shorter wavelengths, the 21 cm radiation has a longer wavelength. This specific wavelength of radiation corresponds to a frequency of approximately 1420 MHz [7].

The 21 cm radiation is significant because it can penetrate interstellar dust and gas clouds, allowing astronomers to study the distribution and dynamics of neutral hydrogen in different cosmic environments. Understanding the properties of neutral hydrogen, which is the most abundant element in the universe, provides valuable insights into the structure and evolution of galaxies.

In this research, the method of drift scans is used to collect the 21 cm radiation and is utilized to conduct analysis of Sun scans, Cas A scans, and the 21 cm spectrum. A galactic scan is used to derive a rotation curve of the Milky Way.

The method of drift scans involves recording separate "passes" of celestial objects such as the Sun and the supernova remnant Cassiopeia A (Cas A). A drift scan is also used to study the 21 cm spectrum, which examines the radiation emitted at different frequencies within the 21 cm wavelength range.

The method of galactic scan uses spectroscopy to measure the velocities of tracer objects, such as stars or gas clouds across the Milky Way. By analyzing the Doppler shifts in their spectra and determining their distances, astronomers can plot the rotational curve of the Milky Way, showing how the orbital velocity changes with distance from the galactic center. This curve provides insights into the galaxy's mass distribution and the presence of dark matter.

1.3. Goals

The objective of this essay is to investigate how 21 cm radiation and the examination of galactic rotation curves contribute to our understanding of galactic dynamics and the distribution of neutral hydrogen. Emphasizing the use of the TLM18 radio telescope and spectral analysis techniques, this essay examines the theoretical foundations, experimental methods, and observational results associated with 21 cm radiation. By investigating the rotation curves of galaxies and the properties of neutral hydrogen, this research seeks to deepen our understanding of the structure and evolution of galaxies, shedding light on the dynamics of galactic systems.

1.4. Personal context

Physics has always been my favorite subject in school. Doing experimental physics is always fun and exciting in school, but the school never taught astronomy as it is not really in the curriculum. But looking at the stars and wondering what it is like has always been one of my childhood questions. When I first encountered astronomy, I found myself drawn into the intriguing science exploring the different physics behind it. Exploring all the spectra, rotations, and atoms inside space is both challenging and fun. I am always amazed that we can uncover valuable information about galaxies by analyzing the signals emitted by hydrogen atoms. It is so interesting to examine what the unknown space is like.

2. Materials and Methods

2.1. Apparatus

The main equipment used is the TLM-18 radio telescope, which has an 18-meter parabolic antenna shown in Figure 1. This antenna is located near Belmar, a town close to the New Jersey shore. Initially, it was used for communication with satellites and gained fame for receiving the first weather images from space. After being unused for some time, it has been repurposed for radio astronomy and amateur radio purposes.

Figure 1. TLM-18 radio telescope antenna in WALL, NJ, UNITED STATES
(Quote from https://www.dvidshub.net/image/6807235/tlm-18-antenna)

The TLM-18 antenna is linked to a mount that enables it to have motion in both vertical (altitude) and horizontal (azimuth) directions. It has 10 HP servo drives and position encoders on each axis, which are connected to a computer in the telescope operations building. The telescope can rotate 360 degrees in azimuth and tilt from 5 to 89 degrees in altitude. The control software allows the antenna to follow celestial objects as they move across the sky because of the Earth's rotation. It also enables remote control of the antenna through a network connection.

At the focus of the parabolic dish, there is a feed horn that collects radiation and sends it to a circular waveguide. Inside the waveguide, probes detect the horizontal and vertical components of the signal. These signals are then amplified and filtered by a receiver system at the feed point. They are transmitted through cables to an operation building nearby. In the operations building, the signals are converted to digital format using a B210 Universal Software Radio Peripheral Module (USRP) from Ettus Research. A software-defined radio (SDR) then processes and records the signals. The B210 USRP module includes a GPS receiver for accurate time stamping of the data. The SDR is based on GNU radio, an open-source module set commonly used in the educational community.

The system operates within the frequency range of 1.0 to 2.0 GHz, with most observations conducted in a 10 MHz band centered on 1420 MHz. This frequency corresponds to the 21-cm radio astronomy band. The telescope's beam size at this frequency is approximately 1.0-degree full width at half maximum (FWHM), which represents the diffraction limit of the telescope.

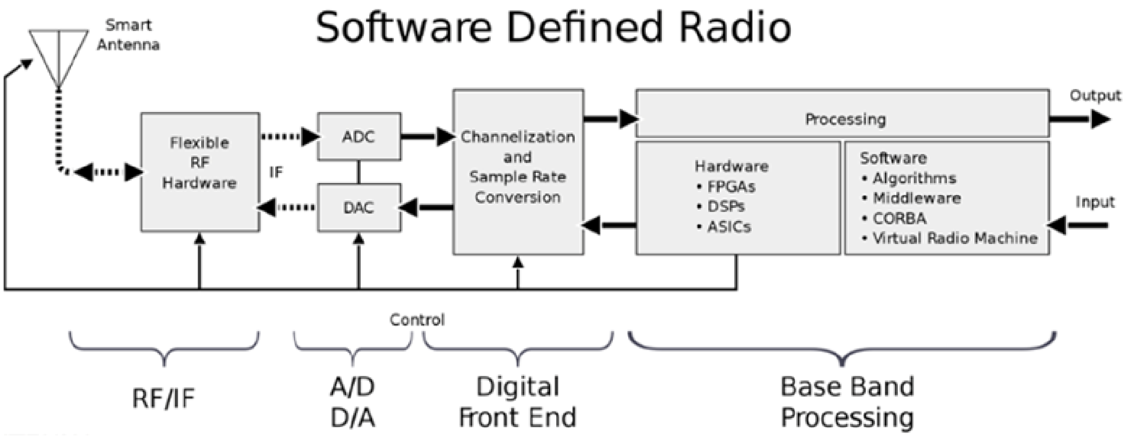

Figure 2. software defined radio structure chart [8]

SDR is a radio technology that uses software instead of complex hardware (shown in figure 2). It allows radios to change their settings, such as frequency and signal processing, through software updates. In it, the necessary hardware is straightforward, and most of the complex work is performed by the computer. In astronomy, SDR is used to study radio signals from space. It offers flexibility and precision in analyzing signals from distant galaxies and other cosmic objects.

The data were collected in March of 2017, using the 18m TLM18 radio telescope in Belmar, New Jersey, USA. The data were collected by the dish operating crew and logged for later analysis.

2.2. Theory Analysis

2.2.1. Angular resolution and Diffraction

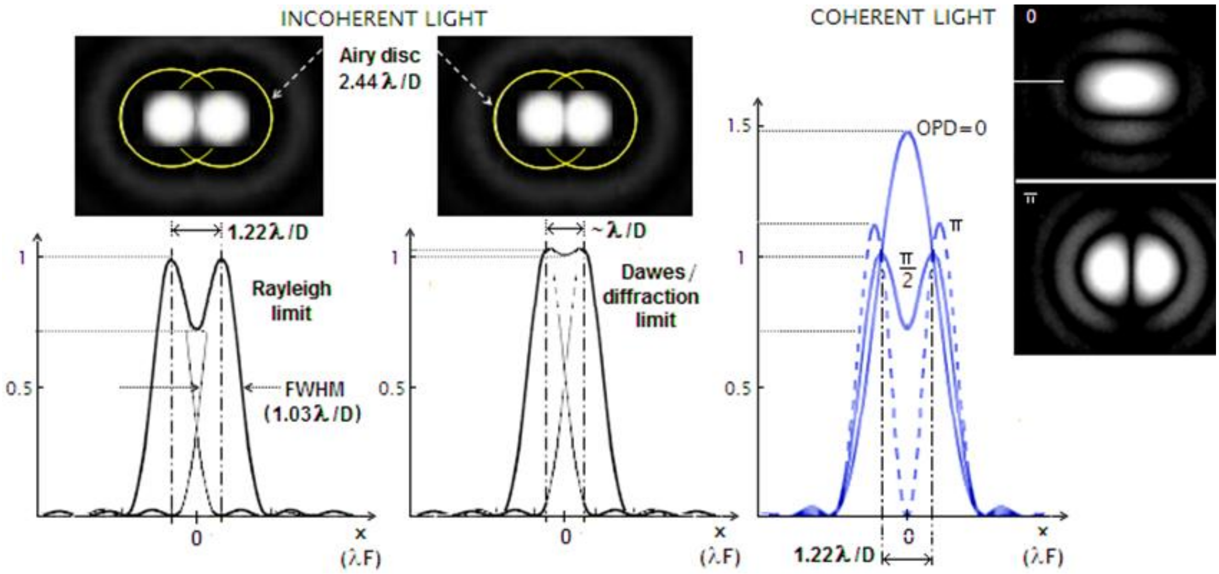

Figure 3. angular resolution of coherent light and incoherent light

(Quote from https: //www.telescope-optics.net/telescope_resolution.htm)

The angular resolution of a telescope is a crucial performance measure that affects its ability to distinguish closely spaced objects in the sky. This concept is illustrated in Figure 3 for an optical telescope. The rightmost sketch demonstrates the blurring effect that occurs when the angular resolution is limited, causing two points to merge into one. Ground-based optical telescopes face various factors that limit their angular resolution, with atmospheric distortion being the most significant, restricting the resolution to around one arc-second.

In contrast, radio astronomy is primarily limited by a phenomenon called "diffraction" rather than atmospheric effects. Diffraction arises from the wave nature of radio signals and imposes a fundamental limit on angular resolution, which can be described by the equation $\Delta\theta = 1.22\lambda/D$. Here, λ represents the wavelength of the telescope's operation, and D refers to the telescope's diameter. For an 18-meter telescope observing at 21 cm wavelength, the angular resolution is approximately 0.8 degrees.

It's important to note that the equations provided yield approximate results. The effective size of the telescope's dish is slightly smaller than the geometric diameter, and other effects can further degrade the resolution.

2.2.2. Spectral Analysis

The term "spectrum" is commonly used both technically and in everyday language. In a technical context, it refers to the range of frequencies present in a signal or wave. To illustrate this concept, let's consider the example of sound, which is more relatable to our everyday experiences.

When a stationary observer listens to sound emitted from a moving source, the apparent frequency of the sound changes based on the relative speed between the source and the observer. An example of this phenomenon is the sound of a passing train's horn or whistle. As the train approaches a stationary observer, the perceived pitch is higher than that heard by an observer on the train. Conversely, as the train moves away, the perceived pitch is lower. This effect, known as the Doppler shift, also occurs in situations like Formula 1 racing, where the sound of the engine's transitions from high to low as the cars pass. Mathematically, this can be expressed as

$$f_{obs} = f_0/(1 - v_s/c) \tag{1}$$

Where f_{obs} Is the Observed Frequency, F0 Is the Emitted Frequency, Vs Is the Speed of The Moving Source (Positive when approaching), and c is the speed of sound. A similar effect can occur if the observer is moving while the sound source remains fixed. The magnitude of the Doppler shift can be significant. For instance, a train moving at 75 mph with a horn pitch of 300 Hz would experience a pitch shift of approximately 10% or 30 Hz. This change in pitch can be easily perceived by the human ear. Importantly, by knowing the exact pitch of the sound source, such as a horn, the speed of the train can be deduced by observing the Doppler shift.

2.2.3. Doppler Shift

The 21 cm line experiences a Doppler shift due to the movement of the observed hydrogen cloud relative to the telescope. If the stars and hydrogen gas in a galaxy were motionless relative to each other, a distinct peak at a frequency of 1420.4 MHz would be observed in the radio spectrum. The intensity of this line varies based on the telescope's direction. Pointing towards the galactic center gives a strong signal, while pointing away in the "thin" direction results in a weaker signal.

The Doppler shift expression is shown in Eq.1

$$f' = \sqrt{\frac{1 + v/c}{1 - v/c}}\, f \simeq (1 + v/c)\, f, \tag{2}$$

Where f is the frequency of the emitted wave, f ' is the observed frequency, v is the relative velocity of approach, and c is the speed of light. Note that when the source and observer are approaching one another, the observed frequency is higher than the emitted frequency.

The galaxy is not a static entity, and its stars are in motion with respect to each other. This leads to an intriguing phenomenon: the 21-cm line is Doppler shifted to different frequencies depending on the relative motion of the observed region in the galaxy. Parts of the galaxy moving towards the observer, exhibit a higher frequency, while parts moving away from the observer produce a lower frequency. This is depicted in Eq.1. It's important to note that the 21-cm line is superimposed on a significant background noise that originates from the receiver. By precisely tracking the frequency of the 21-cm line as a function of direction, astronomers can gain valuable insights into the galaxy and its properties.

2.2.4. Determining and Measuring the Rotation Curve

Determining the rotation curve of a galaxy is a crucial step in investigating the distribution of mass within it. By analyzing the rotational velocities of stars and gas as a function of their distance from the galactic center, astronomers can gain insights into the underlying mass distribution, including the presence of dark matter. Here is a plate demonstrating the rotation:

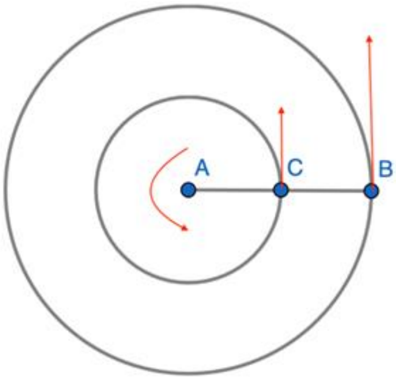

Figure 4. A plate spinning about the axis perpendicular to the plane. Points C and B move with the plate, speed indicated by red arrows.

Calculating rotational velocity requires the velocity of the stars as a function of galactic radius which is $v(r)$. It is then divided into two parts. First, the radius and angular velocity of the sun need to be determined with respect to the galactic center. We initiate these values as r_0 and Ω_0. The velocity of the sun V_0 is given by the angular velocity equation, using

$$v = \frac{2\pi r}{T} = \frac{2\pi r}{(2\pi/\Omega)} = r\Omega \tag{3}$$

Thus $V_0 = v(r_0) = R_0\Omega_0$. To determine the galactic radius depends on the values of R_0 and Ω_0.

The method was found by Dutch astronomer Jan Oort, who introduced the two parameters so that the values could be measured using nearby stars. The value can be measured by observing the stars near the galactic center which at last infers V_0, the orbital velocity of the sun.

The circular velocity of a star at radius r is

$$v(r) = r\Omega(r) \tag{4}$$

The apparent angular velocity of the star is $\Omega(r) - \Omega_0$ so we can change the circular velocity to

$$v' = r\left[\Omega(r) - \Omega_0\right]. \tag{5}$$

All stars located at the same radius relative to the center of the galaxy appear to be fixed with respect to one another. Stars located at radii smaller than the Sun's radius appear to be moving at a velocity v' along the line of sight between the Earth and the star, which is given by

$$v' = r\Omega(r) - r\Omega_0 \Longrightarrow v(r) = r\Omega(r) = v' + r\Omega_0. \tag{6}$$

Knowing that

$$r = R_0 \sin \ell, \tag{7}$$

Where *R0* is the distance from the sun to the center of the galaxy and *l* is the angle between the line of the sun to the star and the sun to the center of the galaxy.

So, Eq. 5 becomes

$$v(r) = v' + R_0\Omega_0 \sin \ell, \tag{8}$$

However, the plane of the galaxy has a wide range of velocity in the same line of direction, and it is not possible to determine which value should be used for v' in Eq.7. thus, we need to substitute Eq.6 into Eq. 5. Which gives

$$v' = R_0 \sin \ell \left[\Omega(r) - \Omega_0 \right] . \quad (9)$$

In summary, finding $v(r)$ is crucial for understanding the rotation curve of the galaxy. It requires knowledge of the parameters R_0 and Ω_0, which were measured by others using nearby stars and careful observations near the galactic center.

3. Results and analysis

3.1. Drift scans

3.1.1. Sun Scan

This analysis focuses on the data obtained from a Sun scan using a drift scan method. The drift scan involves positioning a telescope to point south with an altitude corresponding to the Sun's highest point in the sky. As the Earth rotates, the Sun appears to drift through the telescope's beam, creating a slow and smooth pan effect.

The data collected in this analysis is in a time series format and is processed using Python code. The main objective is to analyze the power detected by the telescope as a function of time during the sun scan.

Plots are generated to display the power detected by the telescope over time. The start and stop times of the data are determined based on the header information, and the time values in between are calculated using the NumPy Lin space function. The resulting plots help visualize the variation of power as the Sun drifts through the telescope's beam.

The graph below (Figure 4), shows a graph comparing the Airy function (the theory model) with the plotted drift scan model.

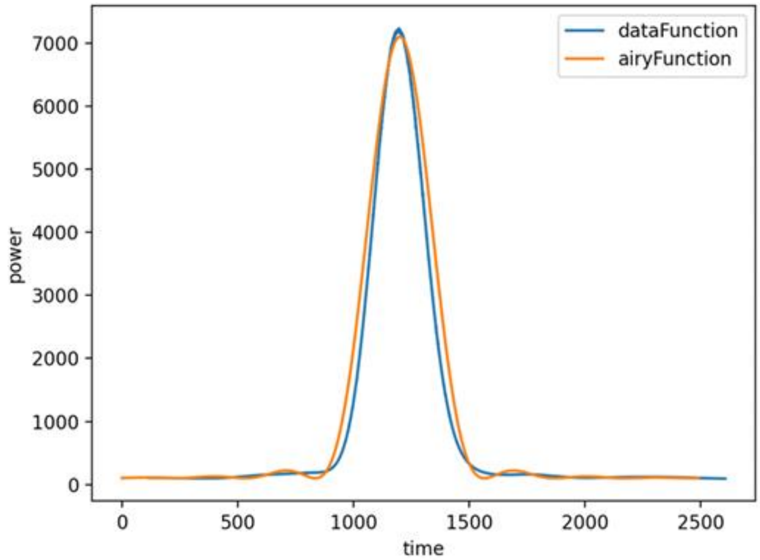

Figure 4. Airy function vs drift scan model plotted in power vs time graph

The Airy function is used in telescope data analysis to describe the point response of the telescope as a function of angle. It characterizes diffraction effects and provides insights into how the telescope focuses light onto a detector or image plane.

The draft scan curve went through several steps including calibrating by dividing the power value by 14300, for present purposes. The obtained values will roughly align with the concept of "antenna temperature," which is a conventional indicator of signal strength in the field of radio astronomy. The curve includes calculations that will require parameters of peak, base, width, and center. The values are set and an argparse function has been used to make setting values more convenient.

At last, instead of plotting the telescope's response over time, we will plot it as a function of angle. This approach will enable us to determine the width of the telescope's beam in degrees. By comparing this value to the predicted value, we can assess their similarity.

$$\Delta\theta = 1.22\frac{\lambda}{D}\ rad = 70°\frac{\lambda}{D} \tag{10}$$

$\lambda = 21\ cm$ is the wavelength and D is the effective diameter of the dish. The equation is added to work out the angle of the dish.

$$\Delta\theta = \frac{d\theta}{dt}\Delta t \simeq \cos\delta\left(\frac{15°}{\mathrm{hr}}\right)\Delta t = \cos\delta\left(\frac{(4.167\times10^{-3})°}{\mathrm{s}}\right)\Delta t \tag{11}$$

During a drift scan, the telescope's beam moves steadily across the sky as the Earth rotates. For a target object at the celestial equator (declination of zero or δ in the equation), the angle between the beam and the target changes at a rate of about 15 degrees per hour. However, for targets at different declinations, we need to adjust the rate of change using a correction factor, roughly corresponding to the cosine of the declination. This correction factor compensates for the varying rates of change in the angle between the beam and targets at different declinations.

In this context, $\Delta\theta$ represents the angular displacement from the center of the peak, Δt is the time offset from the center of the peak, δ denotes the declination, and $d\theta/dt$ represents the rate at which the angle changes over time.

After putting everything together, we can examine the graph, showing that the value of drift scan model is close to the predicted value, with a slight shift to the other side. The power is at its peak during the interval 1000-1500 showing the maximum intensity it could reach which is about 6000-7000 in power.

3.1.2. Cas A scan

The purpose of conducting a Cas A scan is to obtain data and measurements from the supernova remnant for scientific analysis. By performing a drift scan, astronomers can observe the radio emissions from Cas A over a period of time as the Earth rotates. This allows them to collect information about the remnant's radio emission properties, such as its flux density and spectral characteristics.

Similar to the Sun scan, the data collection method used is a "drift scan." The telescope will be positioned towards the north at an elevation of 72 degrees. Each day, Cas A will traverse the telescope's beam, and data will be recorded on consecutive days during its passage. This process can be visualized as a slow and seamless panning movement of the telescope.

The telescope performs a scan pattern over the Cas A region. This pattern can be a raster scan, spiral scan, or any other predetermined pattern. During the scan, the telescope moves systematically across the region, collecting intensity measurements at different positions.

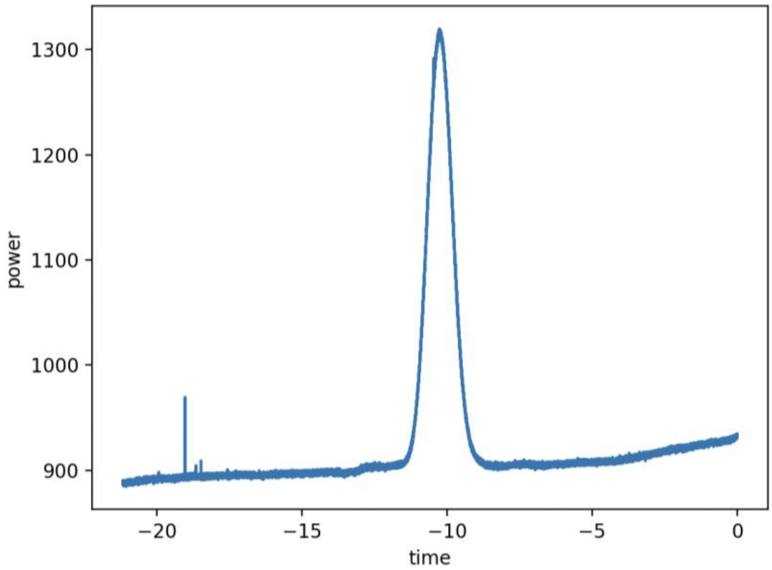

Figure 5. power vs time graph of Cas A scan

In the Sun scan, the background level remained relatively constant. However, in the Cas A-scans, the signal is significantly smaller. Additionally, since Cas A is located within the galaxy, there is a background contribution from galactic emissions. As a result, the background exhibits a slight negative slope. To address this, the code is adjusted to remove the background properly. Instead of subtracting a constant base (or args. base), a straight-line function that follows a specific form is subtracted.

$$B = m\Delta t + b \tag{12}$$

In this context, Δt represents the time difference between the plotted time and the center value (or args. center). The variables m and b respectively denote the slope and the value of the straight-line function.

The result displays a time vs power graph, showing where the Cas A is located within the galaxy. When time is about -10, the intensity is the highest, meaning that the Cas A signal is in that direction. The baseline of the graph is about 900 in power, showing the background signal of the galaxy.

3.2. 21cm spectrum

3.2.1. Raw spectrum

The 21cm spectrum refers to the measurement and analysis of radio waves emitted at a frequency of 1420 MHz, corresponding to a wavelength of 21 centimeters. This frequency range is significant because it is associated with the hyperfine transition of neutral hydrogen (H I). Specifically, it captures the spin-flip transition between the parallel and anti-parallel spins of the electron and proton in a hydrogen atom.

The 21cm line is of great importance in cosmology and astrophysics as it provides valuable information about the distribution and properties of neutral hydrogen in the universe. By studying the 21cm spectrum, researchers can investigate various phenomena, such as the formation of stars, the evolution of galaxies, and the large-scale structure of the cosmos.

We will be examining data collected using the 60-foot telescope. Similar to before, the data was obtained using the "drift scan" method. In this case, the telescope was positioned to face south at an altitude of 45 degrees. The choice of 45 degrees is somewhat arbitrary, but it has proven to produce intriguing outcomes based on past experience. The telescope remained in this position for approximately 40 hours. Each data file represents around 10 minutes of recorded data.

In the first plot, the vertical axis is the power data collected by a dictionary function from a .data file. The horizontal axis represents frequency. The frequency limits for the Fast Fourier Transform (FFT) can be calculated using the following formula:

$$f_{\min} = f_{\text{center}} - \frac{f_{\text{sample}}}{2} \quad \text{and} \quad f_{\max} = f_{\text{center}} + \frac{f_{\text{sample}}}{2}, \tag{13}$$

Where f_{center} represents the center frequency setting, and f_{sample} represents the sampling rate of the digital receiver.

A graph of power vs. frequency is plotted and shown below (Figure 6)

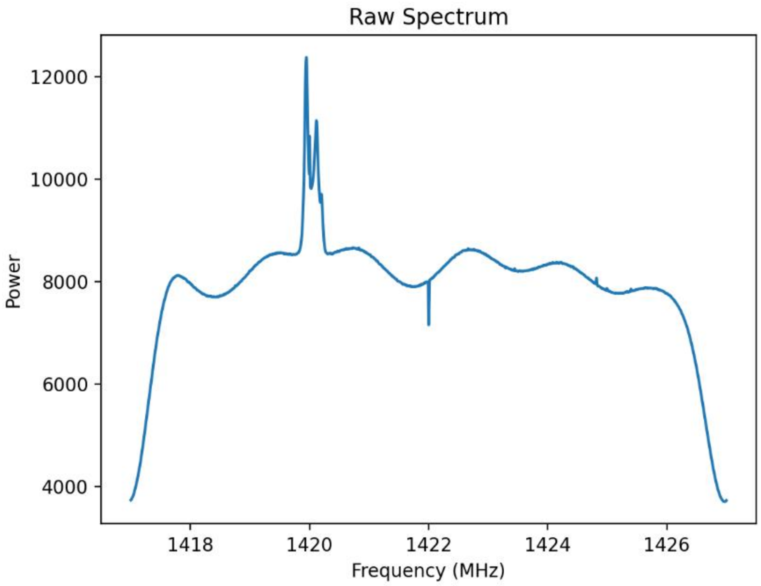

Figure 6. Raw 21cm spectrum plotted in power vs frequency

The new function is created that accepts the previously calculated $freqs$ array and generates a numpy array named vDoppler. The transformation between the values in $freqs$ involves using the known frequency of the 21-cm wave ($f = 1420.41\, MHz$) and the speed of light ($c = 3 \times 105\, km/s$). Ensure that the resulting $vDoppler$ array is arranged in units of kilometers per second (km/s).

A Doppler velocity vs. Power is plotted in Figure 7.

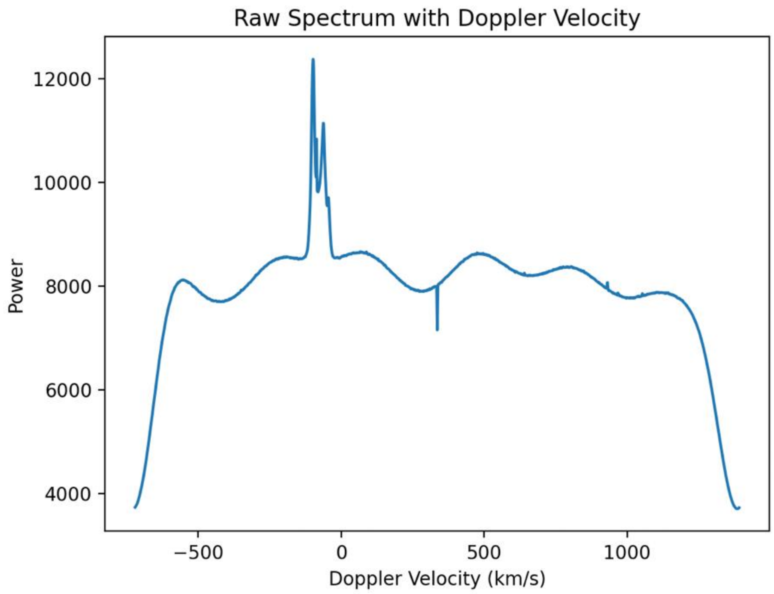

Figure 7. Raw 21cm spectrum plotted in power vs frequency

3.2.2. Gain-corrected spectrum without spurs

When receiving the paper, we assume that the corresponding authors grant us the copyright to use the paper for the book or journal in question. When receiving the paper, we assume that the corresponding authors grant us the copyright to use. We will generate a plot of the gain-corrected spectrum. Additionally, we will identify and eliminate any spurious peaks that may appear at different locations within the spectrum.

This will divide each value of the graph from the "*gain.dat*" file.

The gain correction is implemented on a channel-by-channel basis, following a specific procedure.

$$S_i = \frac{R_i}{G_i} \qquad i = 0, 1, 2, \ldots, 2047 \tag{14}$$

And each value is divided by gain to be corrected such as power:

power = np.divide(power, gain)

Additionally, spurs have to be removed from the graph. To accomplish this, a Python list named "spurChannels" is created that contains the channel numbers corresponding to the spurious peaks.

After selecting and examining the data files, we found that elements 613 to 618 are the spurs, it creates a second maximum to the left of the peak which is incorrect (which can be seen in the previous figure 10 and 11), we must remove it. To do that remove spurs is used for

spurChannels = range (613,618).

Figure 8 is the calibrated graph showing the 21 cm radiation detected at a frequency of 1420MHz, which is like our hypothesis.

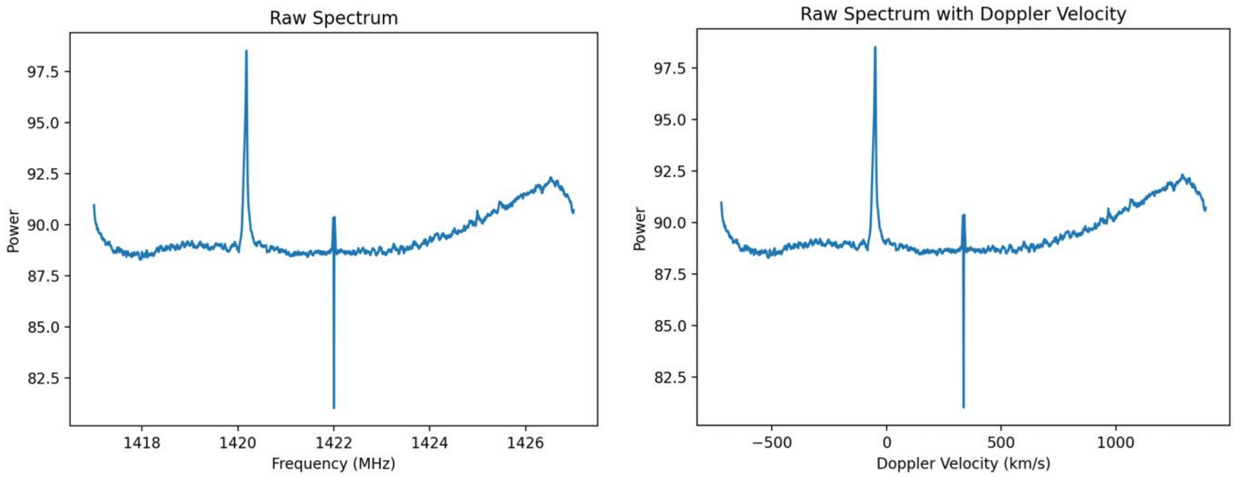

a) b)

Figure 8. a) and b) are figure 6 and figure 7 after gain correction and spurs removal

3.2.3. Spectrum with background subtracted

However, the baseline of the graph is not flat and it contains the background noise. To correct it, we first will subtract the baseline level of the background noise from the data. Second, we will restrict the range of the plot to Doppler velocities within the range of -300 km/s to 300 km/s. Within this range, we will approximate the background as a straight line. The two points used to define this straight line will be the x and y values near the endpoints of the plots, specifically at $vD = \pm 300\ km/s$.

To derive the parameters of a straight line that approximates the noise background between $vD = \pm 300\ km/s$, we can define the background function B with the following functional form:

$$B = m v_D + b, \tag{15}$$

Where B represents the background value at a given Doppler velocity vD, m represents the slope of the line, and b represents the y-intercept.

To determine the parameters m and b, we can use the two points at $vD = \pm 300\ km/s$ as mentioned earlier.

Now, we can calculate the slope m and y-intercept b using the formula: *m* is the slope of the line. $p1$ and $p2$ is the maximum and minimum value of power. $v1$ and $v2$ is the maximum and minimum value of $vDoppler$.

$$m = \frac{p_2 - p_1}{v_2 - v_1} \tag{16}$$

we can determine the parameters *m* and *b*, which will define the straight-line approximation of the noise background within the specified region.

$$b = B_1 - mv_1, \tag{17}$$

The background b is then subtracted from the power array and the plt. Xlim () function is utilized to restrict the horizontal range of the plot to the region encompassing velocities between -300 km/s and 300 km/s.

The result is shown below in Figure 9

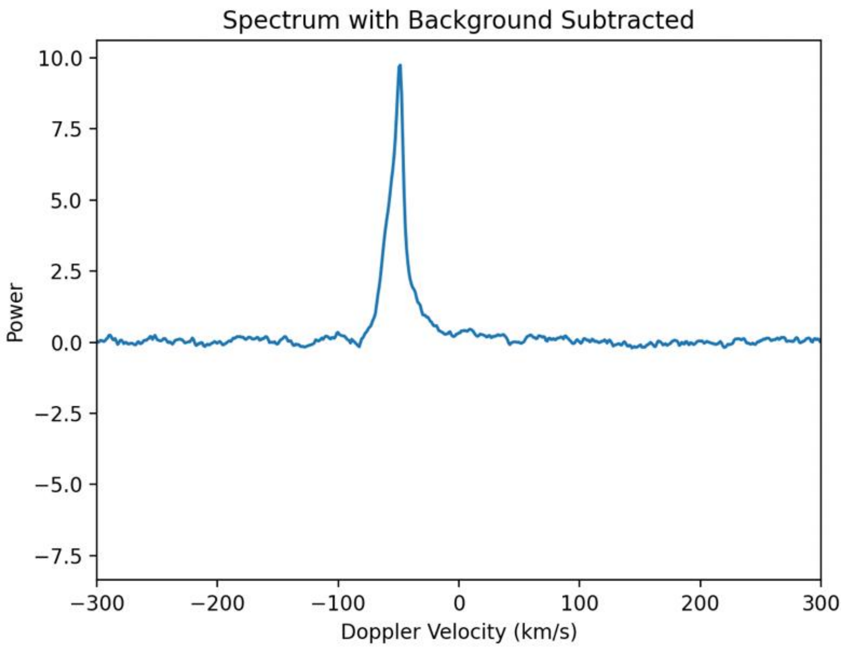

Figure 9. 21cm spectrum with background subtracted, plotted in power vs doppler velocity

The final power vs. Doppler velocity plot provides a visual representation of the power levels at different Doppler velocities Once the calibration process is completed using the gain file and any potential spurious signals are removed from the data, the next steps involve eliminating the background noise and setting the baseline to zero. By examining this plot, we can gain insights into the Doppler velocity of the spectrum when the telescope is pointing in that direction.

3.3. 24-Hour Heat Map

In this part, two-dimensional plots will be generated that depict the Doppler spectrum as a function of time throughout the 24-hour periods corresponding to the 21-cm drift scans. These plots, often referred to as "heat maps," provide a visual representation of the data where color or intensity is used to represent the magnitude of the observed quantity. Heat maps are effective in identifying and highlighting interesting features or patterns within the data, allowing for a comprehensive analysis of the Doppler spectrum variation over time.

Using $np.linspace$ function to plot the graph and k will be a constant value that can be altered from $0.5 < k < 2.0$ for various results. This will then output a heatmap which looks like this (Figure 10)

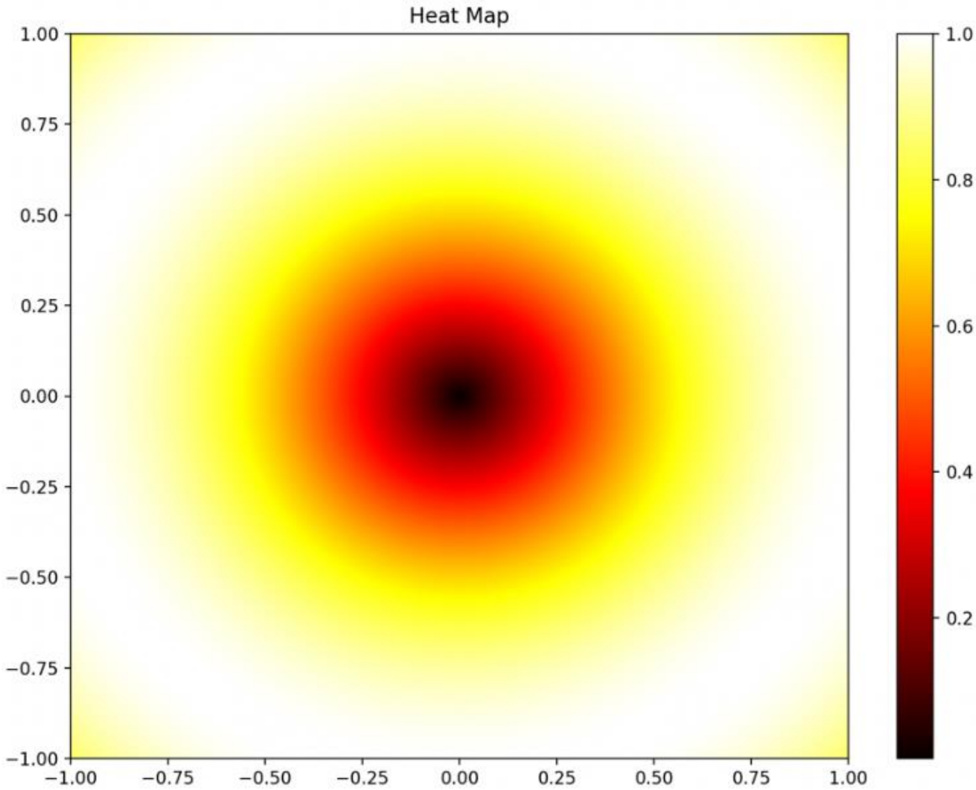

Figure 10. Heat map template for future usage

After getting the appropriate template for a heatmap, a set of real data called *AL045G* from the telescope will be used for the analysis.

To create the heat map, we will arrange it in such a way that the horizontal direction corresponds to Doppler velocity, and the vertical direction corresponds to time. Specifically, we will use the files from the *AL045G* series, where each file in this series will contribute one row to the resulting heat map. This organization allows us to visualize the variation of the Doppler spectrum over time and explore any patterns or trends present in the data.

Instead of calculating the gain ourselves, we can utilize the provided gain file that accompanies each data series. The gain file, named "*AL045G_gain.dat*" contains the necessary 2048 numbers required for the gain correction of individual spectra.

Thus, the gain is fetched from the data files and removed from the power for calibration.

gain = np. from file (“. /data/{0: s}/{0:s}_gain.dat".format(series),dtype=float)

The objective is to estimate the Doppler shift caused by the Earth's motion and indicate the velocity on the plots. However, calculating the velocities involved is a complex task that requires knowledge of various factors such as the time, telescope location, and pointing direction. The direction of the telescope is specified in horizontal coordinates, the Earth's orbital motion is given in equatorial coordinates, and the velocity of the Sun with respect to the Local Standard of Rest (LSR) is typically specified in galactic coordinates.

To simplify this process and avoid the need for installing the pyephem package and performing detailed calculations, a Python module called "*earthVelocityLookup.py*" has been downloaded online. This module assists in calculating the directions and transforming the velocity vectors into equatorial coordinates which saves a lot of time and effort.

In the file all the data is provided and can be used for analysis

'AL045G': [-0.71609172248261288, 28.543485307405071, 57829.221539157268],

An *iDoppler* equation is then sorted onto the graph to create a wave on the heatmap which matches the wave from the 21-cm line.

power[iDoppler] = 35.

After calibrations and setting the timestamp as well as the velocity of the doppler shift. A heat map is shown below (Figure 11)

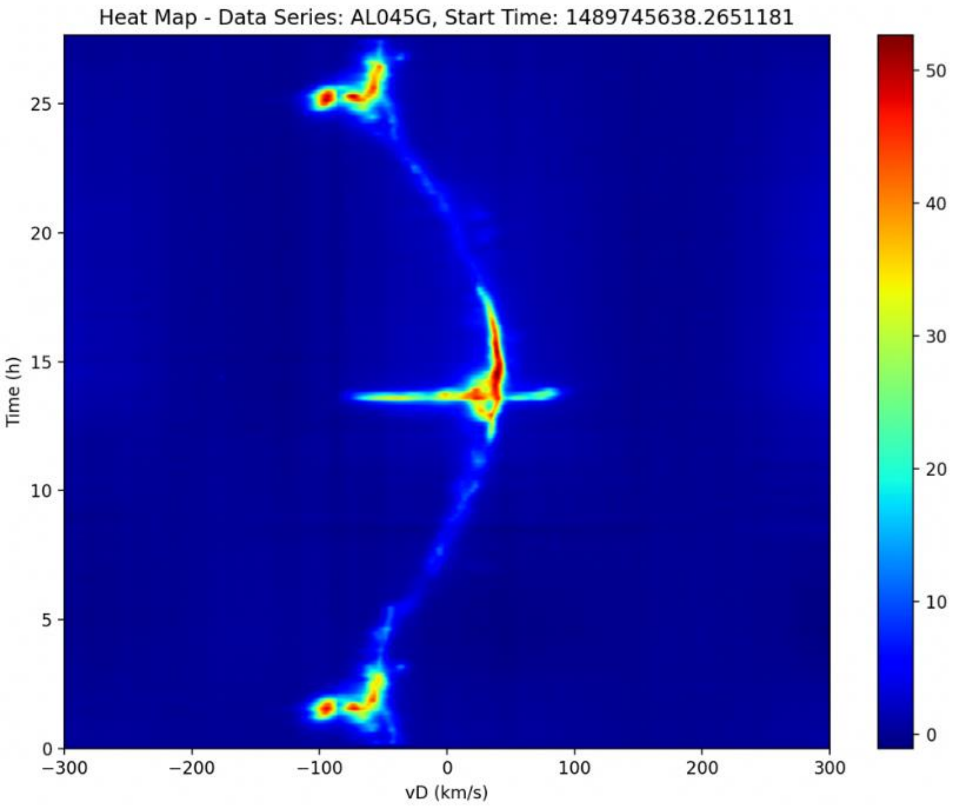

Figure 11. Heat map of the data series AL045G plotted in time vs vDoppler

The color scheme used in the heatmap is "jet," with blue representing a value of 0 and red representing a value of 50. The entire graph appears predominantly blue, indicating lower power levels.

The heatmap exhibits a distinctive pattern resembling a right parenthesis-shaped wave in the middle. The ends of the parenthesis, as well as the middle part, contain three pools of red color, indicating higher power levels. The largest pool of red color is located in the middle section.

On the x-axis, which represents Doppler velocity (vdoppler), both the start and end pools are centered around $-100\ km/s$. This suggests the presence of specific Doppler velocities that exhibit increased power levels at these locations.

In the middle of the graph, there is a large pool of red color, centered around $50\ km/s$ on the x-axis. This indicates a dominant Doppler velocity with the highest power level observed in the dataset.

This means that for the 24-hour period. 21-cm radiation is very intense during the start time (0 and 25) and it is the most intense during the time of 15h, indicating that at that direction there will be more hydrogen atoms or stars.

3.4. Galactic Rotational Curves

To analyze the galactic rotational curves, our objective is to plot the Doppler spectrum as a function of galactic longitude. Additionally, minimum velocity will be extracted from the Doppler spectrum. This minimum velocity value will be corrected for the motion of the Earth and Sun. we will use this corrected value to determine the rotation curve of the Milky Way. This process allows us to study and analyze the rotational motion of our galaxy based on the observed Doppler spectrum and the effects of Earth's and Sun's motion.

In this analysis, data previously obtained using the 60' telescope will be used. Each file in the dataset corresponds to a 120-second observation period where the telescope was fixed on a specific galactic longitude (l) along the galactic equator ($b = 0$). The naming convention for these files will follow the format "gLon022_001.dat," where "gLon022" indicates that the data was captured at a galactic longitude of l = 22°. The "001" at the end of the file name signifies that it is the first run recorded at that particular point.

The code is adjusted to plot vDoppler against galactic longitude instead of vDoppler against time. The glob function is used to retrieve data from the files. Below is the graph of the plotted heat map (Figure 12)

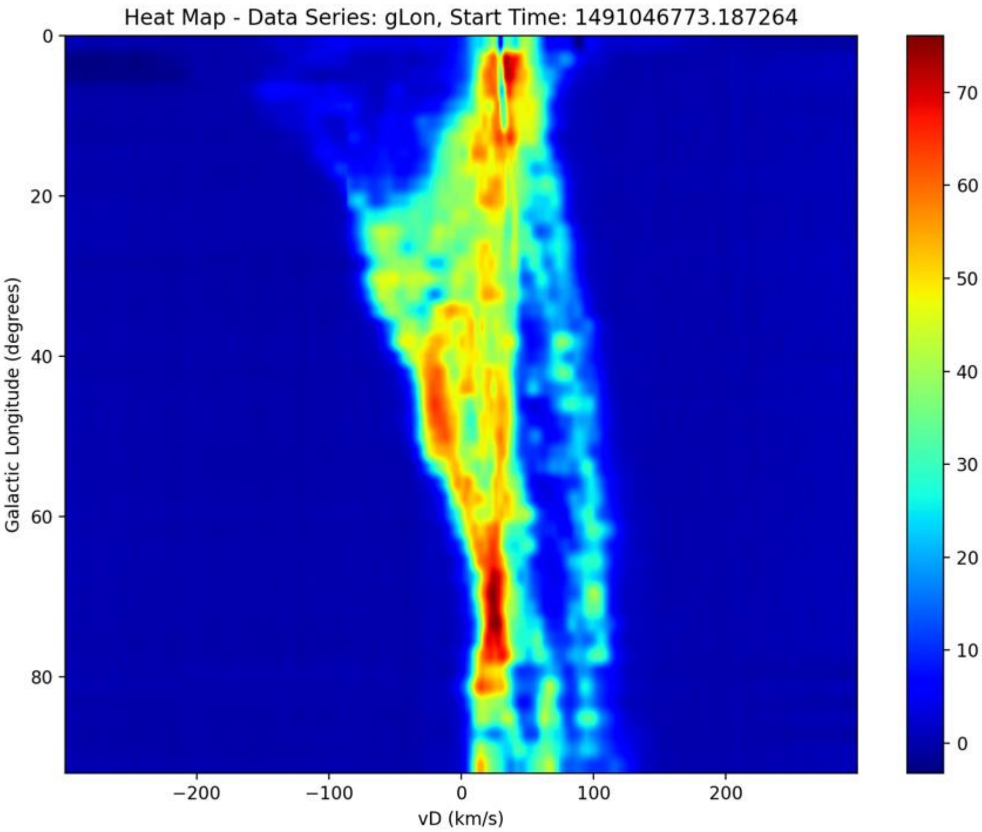

Figure 12. Heat map of the data series gLon plotted in galactic longitude vs vDoppler

The Galactic longitude vs vDoppler graph represents the relationship between the galactic longitude (l) and the Doppler velocity (vDoppler) on the heatmap. Each point on the graph corresponds to a specific galactic longitude and its corresponding Doppler velocity.

The purpose of this graph is to examine the variation of Doppler velocities across different galactic longitudes. By plotting vDoppler against galactic longitude, we can identify any patterns, trends, or structures in the Doppler spectrum that may be correlated with specific galactic locations. In this case we can tell that at 15-25 degrees the heat map has its highest intensity.

In the next steps, an empty Python list called longitude, radius, and vRotation is entered into the graph and plotted.

For each file, these values are appended like:

longitude.append(gLon)

When calculating $vRotation$, utilize the expression for $v(r)$ as provided in the notes on Galactic Rotation.

$$v(r) = v' + R_0\Omega_0 \sin \ell, \tag{18}$$

The corrected version of v', which represents the corrected maximum velocity of recession, is derived from the uncorrected v' value. In this context, $R_0$and $\Omega_0$represent the orbital radius and angular velocity of the Sun, respectively. By subtracting the product of R_0 and Ω_0 from the uncorrected v' value, we obtain the corrected $v'\_corrected$ value, accounting for the effects of the Sun's orbital motion.

$$v'_{\text{corrected}} = -\left(v'_{\text{uncorrected}} - v_{\text{Earth}}\right) = v_{\text{Earth}} - v'_{\text{uncorrected}}, \tag{19}$$

Where $vEarth$ is the value of vDot. The vDots have been scattered on the heatmap below (Figure 13)

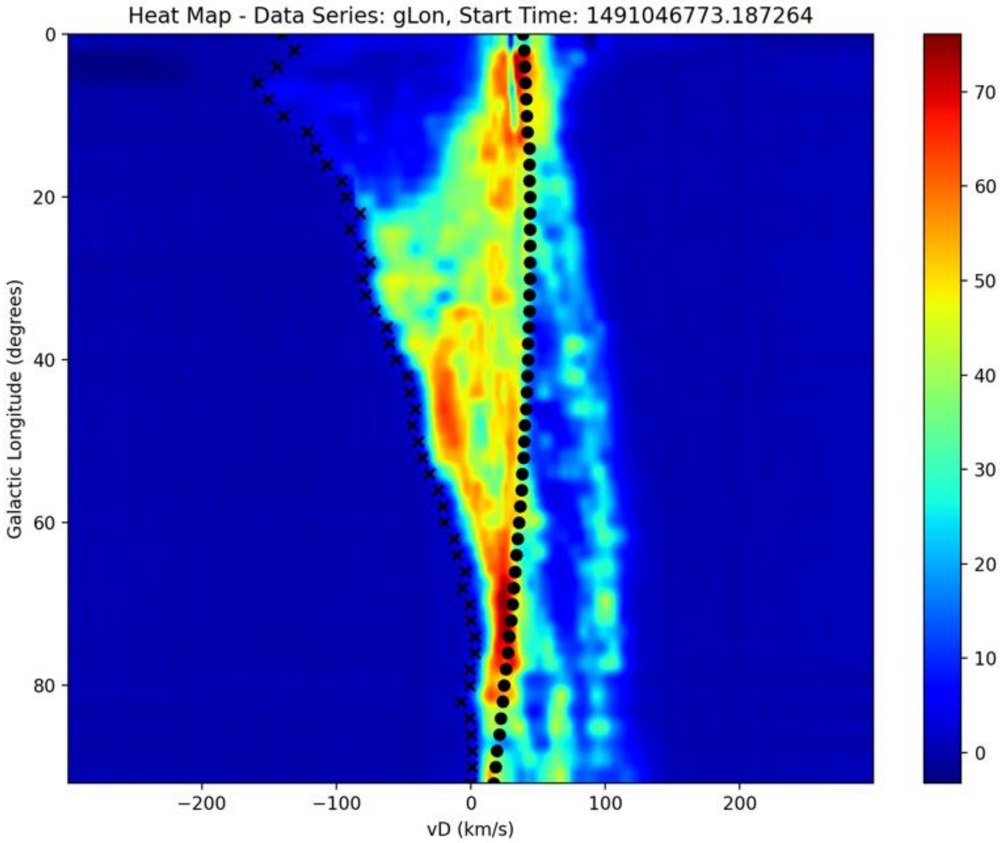

Figure 13. Heat map of the data series gLon plotted in galactic longitude vs vDoppler with a dot representing the vDot line and cross representing the vEdge

The vDot line shows the corrected velocity maximum velocity of recession (vDot) using the galCoords. velocity Projection () function. It is then used to compute the rotational velocity (vRotation) based on the Galactic Rotation equation, accounting for the correction between velocity of approach and velocity of recession. As we can see in the graph, the vDot line outlines the shape of the heat map where the high intensity locates.

And the final use of the data retrieved from before, a rotational velocity versus galactic radius graph has been plotted (Figure 14)

The purpose of plotting the rotational velocity versus galactic radius graph is to visualize the relationship between the rotational velocity of celestial objects and their distance from the galactic center.

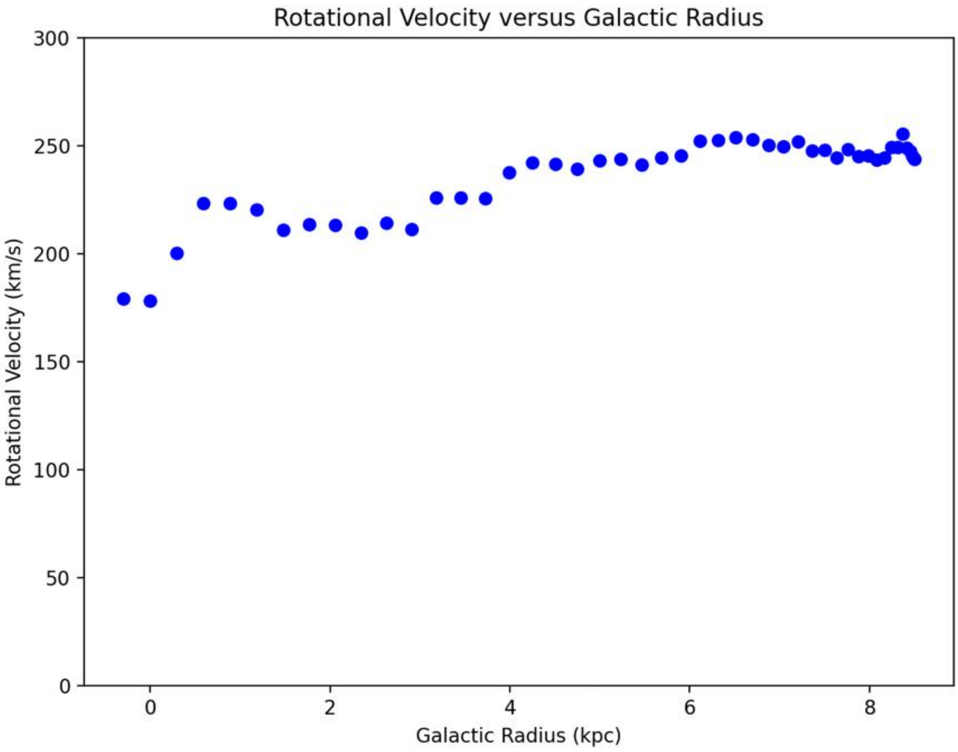

Figure 14. Rotational velocity vs galactic radius relationship

The graph reveals a positive ascending correlation, indicating that as the distance from the galactic center increases (galactic radius), the rotational velocity of objects within the galaxy increases. This pattern is commonly observed in galactic rotation curves.

Notably, the graph exhibits a distinctive feature known as a "flat rotation curve." As the galactic radius reaches around 8 kpc, the gradient of the curve changes, and the rotational velocity appears to level off or remain roughly constant. This phenomenon suggests the presence of dark matter in the galaxy.

Dark matter is an invisible form of matter that does not interact with light but exerts gravitational effects. Its gravitational influence on the outer regions of galaxies causes the observed flat rotation curve. This behavior is a key piece of evidence supporting the existence of dark matter in the universe.

To conclude, the graph provides insights into the rotational dynamics and the distribution of matter, including the presence of dark matter, within the galaxy as a function of galactic radius.

4. Implication and conclusion

4.1. Magnitude of impact

The research conducted on the various data analyses has a significant magnitude of impact on the field of astrophysics as it contributes to our understanding of the rotational dynamics and distribution of matter within galaxies.

By studying the Doppler spectrum variation over time using heat maps, our research provides a comprehensive analysis of the 21-cm radiation from hydrogen atoms or stars in different directions. This analysis allows for the identification of patterns, trends, and intensities of specific Doppler velocities, shedding light on the motion and distribution of matter within the observed region. This information is crucial for understanding the dynamics and structure of galaxies.

Additionally, the research involves analyzing other data such as Sun scans, Cas-A scans, and the galactic rotational curves, which provide insights into the understanding of space. As for the case of the rotational curve, we can examine the rotational motion of celestial objects as a function of their distance from the galactic center. The observation of a flat rotation curve and the negative correlation between rotational velocity and galactic radius indicate the presence of dark matter, a significant finding that supports the existence of this elusive form of matter in the universe.

4.2. Conclusion

Overall, the project serves as an important milestone in the field of galactic astronomy and astrophysics, providing valuable insights into the analysis of diverse data from galaxies. By showcasing the effective utilization of NumPy and Matplotlib for pattern recognition and predicting movements, our research demonstrates a promising future method for studying galactic phenomena. Additionally, the project highlights the ability to discern the direction of entities like Cas A in the vast expanse of the universe, further expanding our knowledge of cosmic structures. Establishing this analytical model can provide scientists with a framework to explore and decipher the complexities of galaxies using advanced computational techniques. This not only enhances our comprehension of galactic dynamics but also paves the way for new discoveries and breakthroughs in the study of the cosmos.

Acknowledgement

Thank you, Mr. Marlow, a physics professor, for introducing me to the subject of astronomy, kindling my interest and providing a significant amount of help such as data collection and data analysis using Python libraries. Mr. Cairns, my physics teacher, for clarifying key concepts, along with helping with the submission process.

References

[1] Blumenthal G R, Faber S M, Flores R, et al. Contraction of dark matter galactic halos due to baryonic infall [J]. Astrophysical Journal, 1985, 301.

[2] Clowe D, Brada, M, Gonzalez A H, et al. A direct empirical proof of the existence of dark matter [J]. Astrophysical Journal, 2006, 648 (2): L109 - L113.

[3] Sirichai C, Joseph S. The 21cm radiation from minihalos as a probe of small primordial non-Gaussianity [J]. Monthly Notices of the Royal Astronomical Society Letters, 2012, 426 (1): L21 - L25.

[4] Ghosh A, Prasad J, Bharadwaj S, et al. Characterizing foreground for redshifted 21cm radiation: 150MHz Giant Metrewave Radio Telescope observations [J]. Monthly Notices of the Royal Astronomical Society, 2012, 426 (4).

[5] VeldkampG. R., Rotation Curves [J]. Journal of Mechanisms, 1967, 2 (2): 147 - 156.

[6] Kent, S, M. Dark matter in spiral galaxies. I - Galaxies with optical rotation curves [J]. The Astronomical Journal, 1986, 91 (6): 1301 - 1301.

[7] Furlanetto S. R., Sokasian A., Hernquist L. Observing the Reionization Epoch Through 21 Centimeter Radiation [J]. Monthly Notices of the Royal Astronomical Society, 2010, 347 (1): 187 - 195.

[8] https: //upcommons.upc.edu/bitstream/handle/2117/78388/109143.pdf.